PHYSICS AND CHEMISTRY OF SOLID STATE
V. 25, No. 3 (2024) pp. 506-512
Section: Physics

DOI: 10.15330/pcss.25.3.506-512

Vasyl Stefanyk Precarpathian National University

ФІЗИКА І ХІМІЯ ТВЕРДОГО ТІЛА
Т. 25, № 3 (2024) С. 506-512
Фізико-математичні науки

PACS: 81.05.Bx, 81.40.Ef, 82.45.Bb, 61.05.cp, 68.37.-d

ISSN 1729-4428 (Print)
ISSN 2309-8589 (Online)

V.A. Polonskyy[1], O.I. Kushnerov[1], V.F. Bashev[2], S.I. Ryabtsev[1]

The Influence of the Cooling Rate on the Structure and Corrosion Properties of the Multicomponent High-Entropy Alloy CoCrFeMnNiBe

[1]*Oles Honchar Dnipro National University, Dnipro, Ukraine, kushnrv@gmail.com*
[2]*Dnipro State Technical University, Kamianske, Ukraine, bashev_vf@ukr.net*

Samples of the multicomponent high-entropy alloy CoCrFeMnNiBe were obtained by the methods of casting and melt-quenching, and their phase composition and electrochemical behavior were investigated. With the help of X-ray phase analysis, it was established that the studied alloy in the as-cast state has a multiphase structure, in which there are phases with lattices of the FCC, BCC, and BeNi(Co) intermetallics (structural type B2). Quenching from the melt leads to a significant decrease in the BCC phase content. The values of stationary potentials and areas of electrochemical stability of cast and melt-quenched CoCrFeMnNiBe alloy samples, as well as corrosion current densities, were determined. It is shown that all samples of the CoCrFeMnNiBe alloy behave inertly in corrosion tests, which allows them to be considered corrosion-resistant. The results of the work can be used in the development of modern multifunctional and corrosion-resistant materials.

Keywords: high-entropy alloy, beryllium, structure, phase composition, electrochemical properties, corrosion resistance.

Received 23 February 2024; Accepted 11 August 2024.

Introduction

In the last two decades, there has been a rapid increase in the number of scientific works devoted to the preparation and study of the properties of the so-called multicomponent high-entropy alloys (HEAs). Such alloys must contain five or more elements in relatively high concentrations (from 5 to 35 at.%). The main difference between HEAs and traditional alloys is that they have a high mixing entropy ΔS_{mix}, which significantly affects their structure and properties [1-4]. The structure and phase composition of various high-entropy alloys can differ significantly from each other. According to the initial concept, HEA should consist only of simple substitutional solid solutions with body-centered (BCC) and face-centered (FCC) cubic lattices, but further studies have shown that such alloys can have a complex structure that is a mixture of different phases, including intermetallic and amorphous [1-10]. Due to high hardness and wear resistance, resistance to ionizing radiation, biocompatibility, and corrosion resistance, high-entropy alloys are promising materials for various fields of engineering [1-4].

The application of quenching from the liquid state with melt cooling rates of 10^5 - 10^6 K/s makes it possible to obtain new metastable states in alloys, including highly supersaturated solid solutions, metastable intermediate phases, in particular the solid amorphous state, with improved physical properties. Thus, quenching from the melt is a promising method for the production of high-entropy alloys [11].

Particularly valuable should be considered such high-entropy alloys that combine improved physical and mechanical properties with sufficiently high corrosion resistance [1-4, 12]. A rather detailed review of the corrosion behavior of various HEAs in comparison with aluminum, nickel, titanium alloys, and stainless steel is given in the works [13, 14]. The investigated media are 3.5 %, 0.6 M, and 1.0 M solutions of NaCl and 0.5 M H_2SO_4. The review [14] summarizes research on

corrosion-resistant HEAs, considers the influence of environments, alloying elements, and analyzes in detail the effect of processing methods on the corrosion resistance of HEAs. In work [15], the corrosion behavior of a single-phase, face-centered cubic high-entropy alloy $Al_{0.1}CoCrFeNi$ in the as-cast state was investigated using the methods of voltammetry and electrochemical impedance spectroscopy, and the obtained results were compared with the corrosion of SS304 steel. The same methods were used in [16] to study the microstructure and corrosion behavior of the CrMnFeCoNi alloy. It was shown that in solutions of 3.5 % NaCl and 0.5 M H_2SO_4, the alloy shows even higher corrosion resistance than stainless steel SS304.

In work [17] the corrosion behavior of the FeCoNiCrMn alloy was studied, the corrosion current densities in solutions of different acidity were determined: - 0.778 μA/cm^2 (1M KOH); 0.879 μA/cm^2 (3.5 % NaCl); 32.9 μA/cm^2 (1M HCl).

Multicomponent single-phase HEA CoCrFeMnNi (Cantor alloy) is one of the most studied HEA [1-3, 7, 18-21]. At the same time, beryllium is a promising element for use in HEAs, considering its physical characteristics such as high hardness and low density [22]. In this work, based on the well-known Cantor alloy CoCrFeMnNi, we obtained a new high-entropy alloy CoCrFeMnNiBe and investigated the effect of rapid quenching from the melt on its structure, as well as corrosion and electrochemical characteristics.

I. Materials and methods

As-cast samples of high-entropy alloys of equiatomic composition $Co_{16.67}Cr_{16.67}Fe_{16.67}Mn_{16.67}Ni_{16.67}Be_{16.67}$ and $Co_{20}Cr_{20}Fe_{20}Mn_{20}Ni_{20}$ (at.%) were obtained using a Tamman high-temperature electric furnace in an argon flow. The average cooling rate when using a copper mold was ~ 10^2 K/s. To ensure homogeneity, the obtained samples were remelted at least three times. After that, a part of the cast samples was used for the production of melt-quenched (MQ) films. The melt quenching method used in this work involves the spreading of a drop of melt, which was shot with the help of a jet of high-pressure inert gas, on the inner surface of a hollow copper cylinder with high thermal conductivity, which rotated at a high speed (~ 8000 rpm). The cooling rate was estimated by the formula $V = \frac{\alpha\vartheta}{c\rho\delta}$. Here c is the heat capacity of the film, ρ is the density of the film material, α is the coefficient of thermal conductivity, ϑ is the excess temperature of the film, and δ is the film thickness [11]. Since the thickness of the obtained MQ films was ~ 40 μm, the estimated cooling rate was ~ 10^6 K/s. X-ray diffraction (XRD) analysis of as-cast samples and MQ films was performed on a DRON-2.0 diffractometer in a monochromatized CuK_α radiation. Diffraction patterns were processed using QualX2 qualitative phase analysis software [23].

Electrochemical studies were performed using a PI-50-1 potentiostat and a PR-8 programmer using a three-electrode cell with a volume of 30 ml. Its design made it possible to use a selected area of the polished surface of the alloy sample with an area of 0.1 cm^2 as a working electrode, to which the cell was tightly pressed through a special hole through a rubber gasket. The auxiliary electrode was a platinum plate with an area of 4 cm^2. Silver chloride served as a reference electrode a half-element connected to the cell through a Luggin capillary, filled with a working solution. All potentials are given relative to this electrode. During the polarization measurements, the solution was not stirred. The potential sweep rate is 1 mV/s.

Corrosion properties were determined by the gravimetric method after exposure of the studied alloy samples in NaCl solution for 1 - 8 days. After each day of testing, the samples were washed with distilled water, dried, and weighed on a WA-21 analytical balance with an error of less than 0.1 mg. The condition of the surface of the alloys during the tests was monitored using a Neophot-21 microscope.

Studies of the value of stationary potentials were carried out in a 3.5 % neutral sodium chloride solution. The pH value of the solution was monitored using an EB-74 ionometer and adjusted to a pH value of 7.0 ± 0.1 by adding appropriate alkali or acid. The temperature of the solutions during the experiments was maintained within 20 ± 2 °C.

The methods of electrochemical and corrosion experiments are described in more detail in the works [24, 25].

II. Results and discussion

XRD patterns of as-cast and MQ samples of the CoCrFeMnNiBe alloy and its prototype - the Cantor alloy CoCrFeMnNi are presented in Figure 1.

According to the results of the X-ray phase analysis, it can be stated that the CoCrFeMnNi alloy in the as-cast state has a single-phase structure, in which the FCC phase with the lattice parameter a = 0.3599 nm is present. Only the FCC phase with a = 0.359 nm is also present in the MQ sample. However, there is a change in the mutual intensities of the (111) and (200) diffraction lines, which indicates the influence of the cooling rate on the alloy crystallization process, in particular on the texture formation. The as-cast sample of the CoCrFeMnNiBe alloy contains an FCC phase with parameters a = 0.3598 nm, a BCC phase (a = 0.2872 nm), and a phase of B2-type ordered solid solution BeNi(Co) (a = 0.2616 nm). The MQ sample consists of an FCC phase (a = 0.3579 nm), and a BeNi(Co) phase (a = 0.2610 nm) and also contains a small amount of BCC phase. Thus, taking into account the intensity of the corresponding diffraction maxima (Fig. 2), in the process of quenching from the melt, the content of the substitution solid solution based on the FCC structure in the CoCrFeMnNiBe alloy increases, and the content of the disordered BCC phase decreases. In addition, the parameter of the FCC lattice decreases to a = 0.3579 nm, obviously due to the increase in the content of beryllium, which has a much smaller atomic radius (0.113 nm) compared to the atomic radii of other alloying elements.

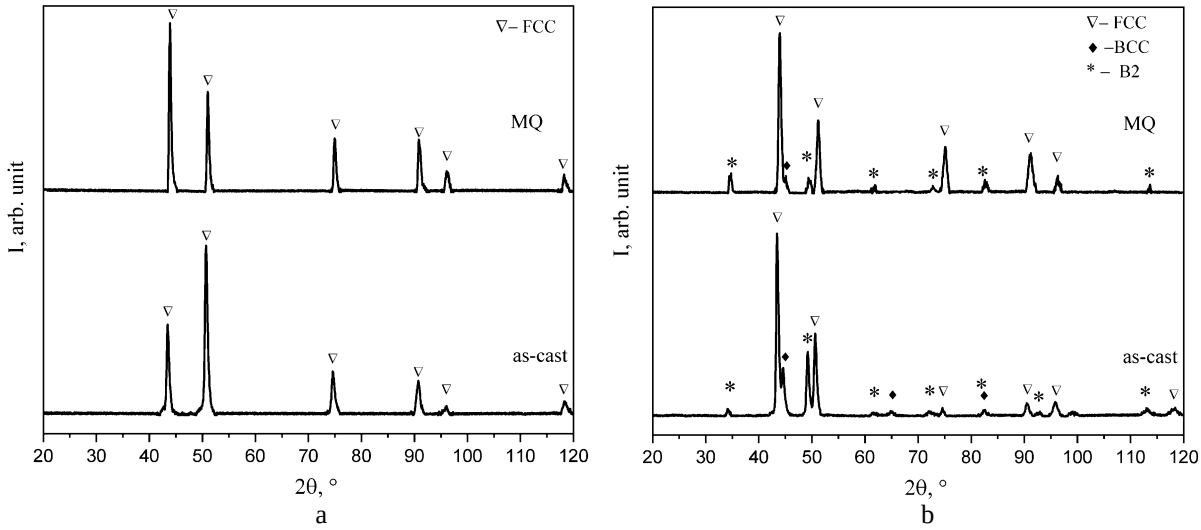

Fig. 1. XRD patterns of as-cast and MQ HEA samples: a - CoCrFeMnNi, b - CoCrFeMnNiBe.

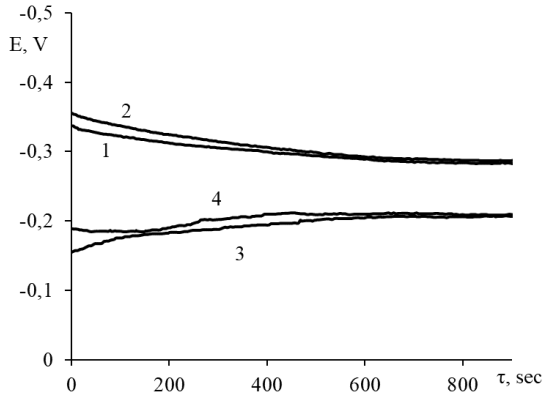

Fig. 2. E, τ – dependences obtained for alloys:
1 – CoCrFeMnNi, 2 – CoCrFeMnNiBe,
3 – CoCrFeMnNi (MQ), 4 – CoCrFeMnNiBe (MQ).

The values of stationary potentials of CoCrFeMnNiBe and CoCrFeMnNi alloys were determined by recording the E, τ - dependences until obtaining an almost unchanged potential value. The obtained results are shown in Fig. 2.

As can be seen at the beginning of the measurements, the values of E in the as-cast alloys differ slightly: – 0.34 V for the CoCrFeMnNi alloy and – 0.35 V for the CoCrFeMnNiBe alloy. A fter approximately 600 seconds of measurements, both potentials acquire a constant value (E_{st} = -0.28 V). MQ samples behave similarly, but the potentials are shifted to more positive values. At the beginning of the measurements, E = -0.18 V for the CoCrFeMnNi (MQ) alloy, and E = -0.15 V for the CoCrFeMnNiBe (MQ) alloy. Gradually, the potential values of these alloys shift slightly to more negative values and acquire a constant value of -0.21 V. Thus, it can be assumed that doping with beryllium and the method of obtaining the alloy does not significantly affect the values of E_{st}.

Polarization studies were performed to determine the zones of electrochemical inertness of the alloy samples studied. In Fig. 3, as an example, a characteristic cyclic voltammogram obtained in a neutral 3.5 % NaCl solution for an as-cast CoCrFeMnNiBe alloy is shown. An anodic sweep of the potential was carried out from the value of

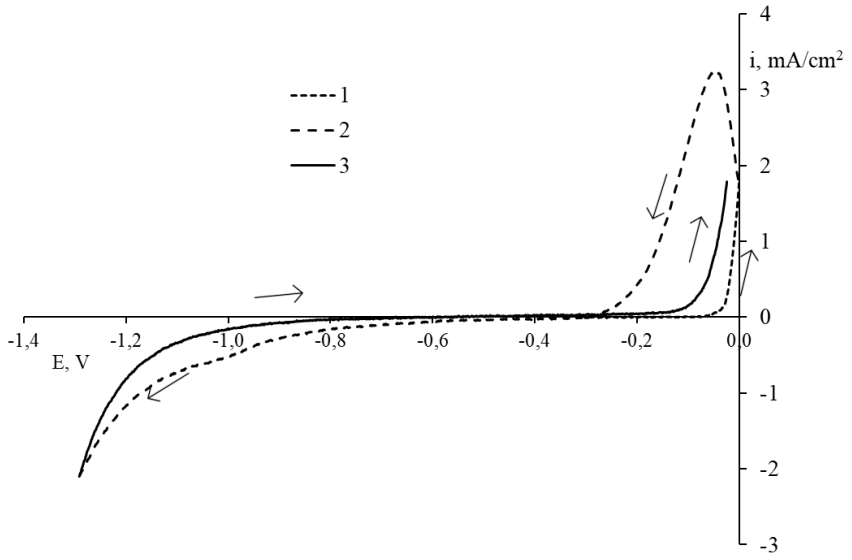

Fig. 3. Cyclic polarization dependence obtained for cast alloy CoCrFeMnNiBe. pH = 7.0; v = 1 mV/s.

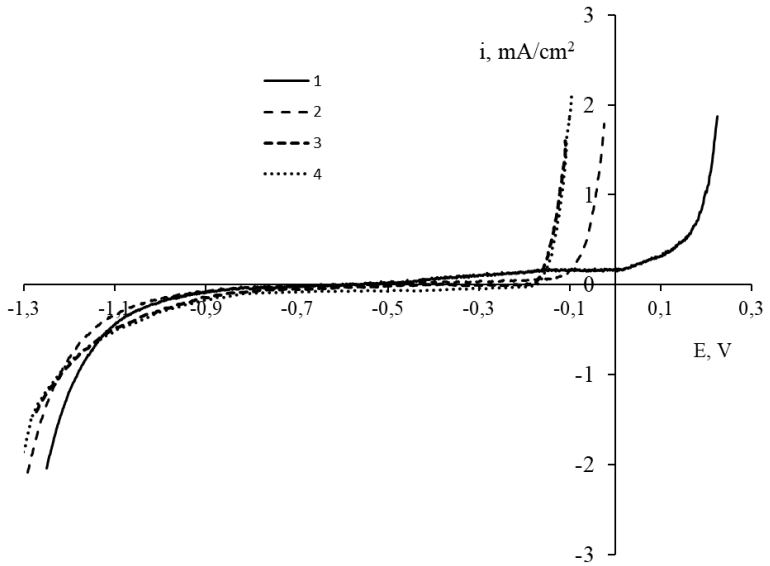

Fig. 4. i, E – dependencies, for alloys: 1 – CoCrFeMnNi, 2 – CoCrFeMnNiBe , 3 – CoCrFeMnNi (MQ), 4 – CoCrFeMnNiBe (MQ).

E_{st} at a speed of 1 mV/s until the beginning of a sharp increase in the current density when active oxidation of the surface of the sample and oxidation of water with the release of oxygen begin to occur. At E = -0.03 V, when i_a = 2 mA/cm^{2,} the direction of the potential sweep changed to the opposite. The zero value of the current density is reached at a potential of -0.30 V. At potential values more negative than -0.8 V, the cathode current density begins to increase, which indicates the beginning of active recovery of the depolarizer, and under such conditions, the surface of the alloy is completely cleaned of oxide films. At E = -1.29 V, when i_k = 2 mA/cm^2, the direction of the potential sweep was changed again, and the zone of electrochemical inertness of the alloy was determined in the third cycle. For the as-cast alloy CoCrFeMnNiBe, it is in the range from -0.8 V to -0.1 V.

Similar cyclic voltammograms were obtained for all investigated alloys. In Fig. 4 shows their i, E - dependences obtained on the third cycle of the potential scan. As can be seen, in the region of negative potentials, all behave inertly up to a potential of 0.8 V, which indicates the same nature of the cathodic process. In the region of positive potentials, the as-cast alloy CoCrFeMnNi is electrochemically inert up to +0.05 V, the alloy CoCrFeMnNiBe – up to -0.1 V, MQ alloys are inert up to -0.15 V.

By processing the obtained i, E - dependences in semi-logarithmic coordinates (Fig. 5) at the intersection points of the tangent to the cathodic and anodic branches of the graph, the values of the corrosion current densities were calculated. It was determined that for the as-cast alloy CoCrFeMnNi $i_{cor} = 7.31 \cdot 10^{-7}$ A/cm^2, and for the CoCrFeMnNiBe alloy $i_{cor} = 2.10 \cdot 10^{-7}$ A/cm^2.

The obtained results are completely correlated with those given for the as-cast CoCrFeMnNi alloy by other authors – $8.79 \cdot 10^{-7}$ A/cm^2 [16].

Values i_{cor} were similarly determined for MQ alloys:

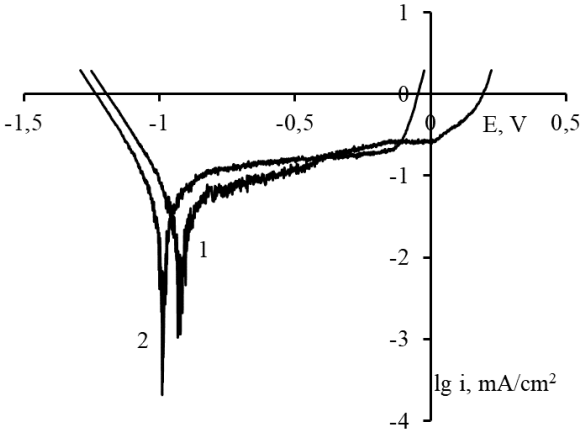

Fig. 5. lg i, E dependence, for the studied as-cast alloys: 1 – CoCrFeMnNi, 2 – CoCrFeMnNiBe.

for the CoCrFeMnNi alloy (MQ) $i_{cor} = 3.83 \cdot 10^{-7}$ A/cm^2, and for the CoCrFeMnNiBe alloy (MQ) $i_{cor} = 2.88 \cdot 10^{-8}$A/cm^2.

The corrosion behavior of as-cast alloy samples was investigated by fully immersing them in a 3.5 % NaCl solution at a temperature of 20 ± 2 °C with periodic monitoring of the surface condition after 1, 2, 4, and 8 days from the start of the experiment. The state of the surface of the samples of the investigated alloys before the tests and after 8 days of the tests are presented in the photomicrographs of Figure 6.

As can be seen, there are no changes in the state of the surface of the samples associated with corrosion processes. Also, for the MQ samples, in the process of corrosion tests, their mass was controlled and it remained unchanged.

The results of model corrosion tests of the studied alloy samples allow us to consider them corrosion-resistant.

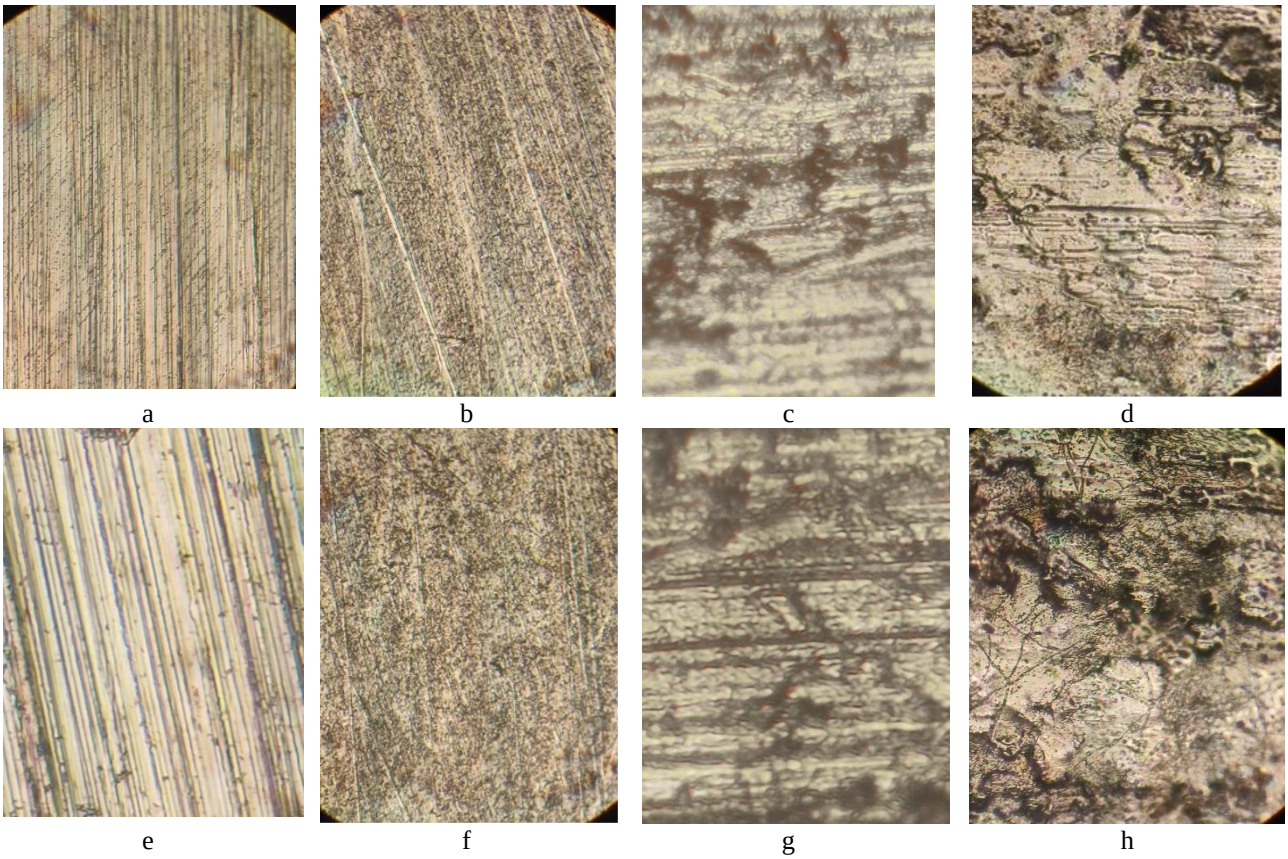

Fig. 6. Surface condition of alloy samples CoCrFeMnNi (a, e), CoCrFeMnNiBe (b, f), CoCrFeMnNi (MQ) (c, g), CoCrFeMnNiBe (MQ) (d, h) during corrosion tests (x1000): a, b, c, d – before tests; e, f, g, h - after 8 days of testing.

Conclusions

According to the results of the X-ray phase analysis of as-cast and quenched from the melt at a speed of ~10^6 K/s samples of the high-entropy alloy CoCrFeMnNiBe, it was established that in the as-cast state the structure of the alloy contains an FCC phase (a = 0.3598 nm), a BCC phase (a = 0.2872 nm) and a phase of B2-type ordered solid solution BeNi(Co) (a = 0.2616 nm). Quenching from the melt contributes to an increase in the content of the FCC phase and ordered phase B2 due to a decrease in the content of the BCC phase.

The values of stationary potentials of CoCrFeMnNi and CoCrFeMnNiBe alloys in the as-cast and MQ state in a neutral 3.5 % NaCl solution were determined. It was found that the addition of Be in Cantor's alloy does not lead to a change in the values of E_{st}. In as-cast alloys the value of E_{st} = -0.28 V, and in MQ alloys E_{st} = -0.21 V.

Based on the results of polarization measurements, the areas of electrochemical stability of the studied alloy samples were determined. In the negative region of the potentials for all investigated alloys, they reach a value of 0.8 V. This indicates the same nature of the cathodic process, which occurs with oxygen depolarization in a neutral sodium chloride solution. In the positive range of potentials, the cast alloy CoCrFeMnNi is the most stable. Its doping with beryllium shifts the boundary of the zone of electrochemical stability from +0.05 V to = -0.1 V. The calculated values of the corrosion current densities are $7.31 \cdot 10^{-7}$ A/cm^2 for the CoCrFeMnNi alloy, $2.10 \cdot 10^{-7}$ A/cm^2 for the CoCrFeMnNiBe alloy, $3.83 \cdot 10^{-7}$ A/cm ^{2} for the CoCrFeMnNi (MQ) alloy and $2.88 \cdot 10^{-8}$ A/cm ^{2} for the CoCrFeMnNiBe (MQ) alloy.

The results of model corrosion tests of all investigated alloy samples carried out in a neutral 3.5 % NaCl solution for 1 - 8 days, allow us to consider them corrosion-resistant. Thus, taking into account the significant improvement in mechanical characteristics that occurs when Be is added to the CoCrFeMnNi alloy, especially during quenching from the melt [22], the studied high-entropy alloy CoCrFeMnNiBe in the as-cast and melt-quenched state is promising for practical applications.

Polonsky V.A. - Ph.D., Associate Professor of the Department of Physical, Organic, and Inorganic Chemistry;
Kushnerev O.I. - Ph.D., Associate Professor of the Department of Experimental Physics;
Bashev V.F. - Dr.Sci, Professor of the Condensed State Physics Department;
Ryabtsev S.I. – Dr.Sci, Head of the Department of Experimental Physics.

[1] T.S. Srivatsan, M. Gupta, *High Entropy Alloys, Innovations, advances, and applications* (CRC Press, Boca Raton, 2020).
[2] H. Xiang, F.-Z. Dai, Y. Zhou, *High- Entropy Materials*. From Basics to Applications, 1st ed. (WILEY- VCH GmbH, Weinheim, Germany, 2023).
[3] J. Brechtl, P.K. Liaw, *High-Entropy Materials: Theory, Experiments, and Applications* (Springer International Publishing, Cham, 2021).
[4] D.B. Miracle, O.N. Senkov, *A critical review of high entropy alloys and related concepts*, Acta Materialia, 122, 448 (2017); https://doi.org/10.1016/j.actamat.2016.08.081.
[5] S.I. Mudry, R.M. Bilyk, R.Y. Ovsianyk, Y.O. Kulyk, T.M. Mika, *Structural features of InPbGaSnCu molten high entropy alloy*, Physics and Chemistry of Solid State, 20(4), 432 (2019); https://doi.org/10.15330/pcss.20.4.432-436.
[6] V.V. Girzhon, V.V. Yemelianchenko, O.V. Smolyakov, A.S. Razzokov, *Analysis of structure formation processes features in high-entropy alloys of Al-Co-Cr-Fe-Ni system during laser alloying*, Results in Materials, 15(June), 100311 (2022); https://doi.org/10.1016/j.rinma.2022.100311.
[7] O.I. Kushnerov, S.I. Ryabtsev, V.F. Bashev, *Metastable states and physical properties of Co-Cr-Fe-Mn-Ni high-entropy alloy thin films*, Molecular Crystals and Liquid Crystals, 750(1), 135 (2023); https://doi.org/10.1080/15421406.2022.2073043.
[8] G.A. Bagliuk, M.V. Marych, Yu.O. Shishkina, A.A. Mamonova, O.M. Gripachevsky, S.F. Kyryliuk, *Features of phase and structure formation in obtaining high-entropy alloy of Fe-Ti-Cr-Mn-Si-C system from a powder mixture of ferroalloys*, Physics and Chemistry of Solid State, 23(3), 620 (2022); https://doi.org/10.15330/pcss.23.3.620-625.
[9] V. Girzhon, V. Yemelianchenko, O. Smolyakov, *High entropy coating from AlCoCrCuFeNi alloy, obtained by laser alloying*, Acta Metallurgica Slovaca, 29(1), 44 (2023); https://doi.org/10.36547/ams.29.1.1710.
[10] M. Dufanets, V. Sklyarchuk, Yu. Plevachuk, Y. Kulyk, S. Mudry, *The Structural and Thermodynamic Analysis of Phase Formation Processes in Equiatomic AlCoCuFeNiCr High-Entropy Alloys*, Journal of Materials Engineering and Performance, 29(11), 7321 (2020); https://doi.org/10.1007/s11665-020-05250-6.
[11] O.I. Kushnerov, V.F. Bashev, *Structure and Physical Properties of Cast and Splat-Quenched CoCr0.8Cu0.64FeNi High Entropy Alloy*, East European Journal of Physics, 48(3), 43 (2021); https://doi.org/10.26565/2312-4334-2021-3-06.
[12] H.C. Ozdemir, A. Nazarahari, B. Yilmaz, D. Canadinc, E. Bedir, R. Yilmaz, U. Unal, H. J. Maier, *Machine learning – informed development of high entropy alloys with enhanced corrosion resistance*, Electrochimica Acta, 476, 143722 (2024); https://doi.org/10.1016/j.electacta.2023.143722.
[13] Z. Tang, L. Huang, W. He, P. Liaw, *Alloying and Processing Effects on the Aqueous Corrosion Behavior of High-Entropy Alloys*, Entropy, 16(2), 895 (2014); https://doi.org/10.3390/e16020895.
[14] Y. Shi, B. Yang, P. Liaw, *Corrosion-Resistant High-Entropy Alloys: A Review*, Metals, 7(2), 43 (2017); https://doi.org/10.3390/met7020043.
[15] N. Kumar, M. Fusco, M. Komarasamy, R. S. Mishra, M. Bourham, K. L. Murty, *Understanding effect of 3.5 wt.% NaCl on the corrosion of Al0.1CoCrFeNi high-entropy alloy*, Journal of Nuclear Materials, 495, 154 (2017); https://doi.org/10.1016/j.jnucmat.2017.08.015.
[16] Q. Ye, K. Feng, Z. Li, F. Lu, R. Li, J. Huang, Y. Wu, *Microstructure and corrosion properties of CrMnFeCoNi high entropy alloy coating*, Applied Surface Science, 396, 1420 (2017); https://doi.org/10.1016/j.apsusc.2016.11.176.
[17] B. Wang, J. Huang, J. Fan, Y. Dou, H. Zhu, D. Wang, *Preparation of FeCoNiCrMn High Entropy Alloy by Electrochemical Reduction of Solid Oxides in Molten Salt and Its Corrosion Behavior in Aqueous Solution*, Journal of The Electrochemical Society, 164(14), E575 (2017); https://doi.org/10.1149/2.1521714jes.
[18] M. Hu, X. Ouyang, F. Yin, X. Zhao, Z. Zhang, X. Wang, *Effect of Boronizing on the Microstructure and Mechanical Properties of CoCrFeNiMn High-Entropy Alloy*, Materials, 16(10), 3754 (2023); https://doi.org/10.3390/ma16103754.
[19] H. Shahmir, P. Saeedpour, M. S. Mehranpour, S. A. A. Shams, C. S. Lee, *Hetero-Deformation Induced Hardening in a CoCrFeNiMn High-Entropy Alloy*, Crystals, 13(5), 844 (2023); https://doi.org/10.3390/cryst13050844.
[20] A.V. Zavdoveev, O.A. Gaivoronsky, V.D. Poznyakov, A.V. Klapatyuk, D.V. Vedel, T. Baudin, O.A. Los, R.A. Kozin, M.A. Skoryk, *Powder Welding Wire of Cantor's High-Entropy Alloying System for Surfacing*, Metallofizika i Noveishie Tekhnologii, 44(8), 1025 (2022); https://doi.org/10.15407/mfint.44.08.1025.
[21] M.P. Semen'ko, R.V. Ostapenko, S.M. Naumenko, P.O. Teselko, *Influence of technological factors on the structure and properties of high-entropy FeCrMnCoNi alloy*, Journal of Nano- and Electronic Physics, 11(6), (2019); https://doi.org/10.21272/jnep.11(6).06017.
[22] V.F. Bashev, O.I. Kushnerov, S.I. Ryabtsev, *Structure and properties of CoCrFeNiMnBe high-entropy alloy films obtained by melt quenching*, Molecular Crystals and Liquid Crystals, 765(1), 145 (2023); https://doi.org/10.1080/15421406.2023.2215125.
[23] A. Altomare, N. Corriero, C. Cuocci, A. Falcicchio, A. Moliterni, R. Rizzi, *Main features of QUALX2.0 software for qualitative phase analysis*, Powder Diffraction, 32(S1), 129 (2017); https://doi.org/10.1017/S0885715617000240.

[24] V.A. Polonskyy, V.F. Bashev, O.I. Kushnerov, *Structure and corrosion-electrochemical properties of Fe-based cast high-entropy alloys*, Journal of Chemistry and Technologies, 28(2), 176 (2020); https://doi.org/10.15421/082019.
[25] V.A. Polonskyy, V.F. Bashev, O.I. Kushnerov, *Structure and corrosion-electrochemical properties of rapidly quenched Fe5CrCuNiMnSi and Fe5CoCuNiMnSi high entropy alloys*, Journal of Chemistry and Technologies, 30, 88 (2022); https://doi.org/10.15421/jchemtech.v30i1.237109.

В.А. Полонський[1], О.І. Кушнерьов[1], В.Ф. Башев[2], С.І. Рябцев[1]

Вплив швидкості охолодження на структуру та корозійні властивості багатокомпонентного високоентропійного сплаву CoCrFeMnNiBe

[1]*Дніпровський національний університет імені Олеся Гончара, м. Дніпро, Україна, kushnrv@gmail.com*
[2]*Дніпровський державний технічний університет, м. Кам'янське, Україна, bashev_vf@ukr.net*

В роботі методами лиття та гартування з розплаву отримані зразки багатокомпонентного високоентропійного сплаву CoCrFeMnNiBe, досліджено їх фазовий склад та електрохімічну поведінку. За допомогою рентгенофазового аналізу встановлено, що досліджуваний сплав у литому стані має багатофазну структуру, в якій присутні фази із ґратками типу ГЦК, ОЦК та інтерметаліди BeNi(Co) (структурний тип B2). Гартування з розплаву призводить до значного зменшення вмісту ОЦК фази. Визначені величини стаціонарних потенціалів та області електрохімічної стабільності литих та загартованих з розплаву зразків сплаву CoCrFeMnNiBe, а також густини струмів корозії. Показано, що усі зразки сплаву CoCrFeMnNiBe в корозійних випробуваннях поводять себе інертно, що дозволяє вважати їх корозійно тривкими. Результати роботи можуть бути використані при розробці сучасних багатофункціональних та корозійно тривких матеріалів.

Ключові слова: високоентропійний сплав, берилій, структура, фазовий склад, електрохімічні властивості, корозійна тривкість.